

Demixing and orientational ordering in mixtures of rectangular particles

D. de las Heras*

Departamento de Física Teórica de la Materia Condensada, Universidad Autónoma de Madrid, E-28049 Madrid, Spain

Yuri Martínez-Ratón†

Grupo Interdisciplinar de Sistemas Complejos (GISC), Departamento de Matemáticas, Escuela Politécnica Superior, Universidad Carlos III de Madrid, Avenida de la Universidad 30, E-28911 Leganés, Madrid, Spain

Enrique Velasco‡

Departamento de Física Teórica de la Materia Condensada and Instituto de Ciencia de Materiales Nicolás Cabrera, Universidad Autónoma de Madrid, E-28049 Madrid, Spain

(Received 7 May 2007; published 7 September 2007)

Using scaled-particle theory for binary mixtures of two-dimensional hard particles with orientational degrees of freedom, we analyze the stability of phases with orientational order and the demixing phase behavior of a variety of mixtures. Our study is focused on cases where at least one of the components consists of hard rectangles, or a particular case of these, hard squares. A pure fluid of hard rectangles has recently been shown to exhibit, aside from the usual uniaxial nematic phase, an additional oriented phase, called tetratic phase, possessing two directors, which is the analog of the biaxial or cubatic phases in three-dimensional fluids. There is evidence, based on computer simulation studies, that the tetratic phase might be stable with respect to phases with lower translational symmetry for rectangles with low aspect ratios. As hard rectangles are mixed, in increasing concentration, with other particles not possessing stable tetratic order by themselves, the tetratic phase is destabilized, via a first- or second-order phase transition, to uniaxial nematic or isotropic phases; for hard rectangles of low aspect ratio (hard squares, in particular), tetratic order persists in a relatively large range of volume fractions. The order of these transitions depends on the particle geometry and dimensions, and also on the thermodynamic conditions of the mixture. The second component of the mixture has been chosen to be hard disks or discorightangles, the geometry of which is different from that of rectangles, leading to packing frustration and demixing behavior, or simply rectangles of different aspect ratio but with the same particle area, or different particle area but with the same aspect ratio. These mixtures may be good candidates for observing thermodynamically stable tetratic phases in monolayers of hard particles. Finally, demixing between fluid (isotropic-tetratic or tetratic-tetratic) phases is seen to occur in mixtures of hard squares of different sizes when the size ratio is sufficiently large.

DOI: [10.1103/PhysRevE.76.031704](https://doi.org/10.1103/PhysRevE.76.031704)

PACS number(s): 64.70.Md, 64.75.+g, 61.20.Gy

I. INTRODUCTION

Mixtures of three-dimensional rodlike molecules have been analyzed quite extensively, both experimentally and theoretically [1]. Beautiful experiments on molecular and colloidal particles have been reported, with the observation of different phases, such as isotropic and nematic phases of various kinds [2]. Of special interest is the issue of orientational phase transitions and, in particular, of entropically driven phase segregation in these systems, a long-debated question in the context of hard spheres [3]. There is now ample theoretical evidence for segregation and demixing phenomena in hard-core mixtures of anisotropic particles [4–9]. Particularly interesting are segregation phenomena between two nematic phases, which sometimes show upper critical points [10]. More recently, the occurrence and overall influence of spatially ordered phases, in the perfect-alignment approximation, have been analyzed [9,11], and

more complete studies, lifting the latter approximation, on the effect of layered phases and microsegregation phenomena on the phase behavior have been carried out [12–14].

Studies on the corresponding two-dimensional mixtures are very scarce. In Ref. [15] it was shown that two-dimensional isotropic mixtures of hard convex bodies can never demix within scaled-particle theory (SPT). A unimodal polydisperse mixture of hard needles was also studied within the Onsager approach in Ref. [16], one result being that the isotropic-nematic transition is always of second order. Also, an equation of state for two-dimensional mixtures of hard bodies has been constructed starting from an approximation for their direct correlation functions [17]; it was found that demixing never occurs. Finally, a theoretical study has recently been carried out for mixtures of hard rectangles and discorightangles within the framework of SPT [18]. Using a bifurcation analysis, demixing between different phases, one of which is an orientationally ordered phase, was shown to occur.

The analysis of this problem is sufficiently motivated by the importance of surface-phase transitions experienced by monolayers of adsorbed molecules. But, since the transition from the disordered phase to the oriented (nematic) phase in one-component fluids may be, and in most cases is, of sec-

*daniel.delasheras@uam.es

†yuri@math.uc3m.es

‡enrique.velasco@uam.es

ond order in two dimensions, many new interesting features may arise in the phase diagram of the mixture, such as tricritical and critical end points, which are absent in three dimensions. Our recent work on two-dimensional hard-rod fluids [18] has demonstrated that these systems do in fact exhibit a richer phase behavior, with the additional fact that, due to spatial restrictions, phase behavior may be more sensitive to subtle effects associated with the particle geometrical shapes. It would be desirable to understand the differences and similarities between the two dimensionalities and elucidate their origin.

In fact, liquid-crystalline phase transitions in one-component fluids depend strongly on dimensionality. A general trend of two-dimensional systems with continuous symmetry is the lack of true long-range order [19], which in a two-dimensional nematic would be reflected in the presence of quasi-long-range orientational order [20–24]. Thus, in the absence of any other mechanism, transitions from the isotropic phase (I) to the uniaxial nematic phase (N_u) in two-dimensional, one-component fluids of hard rods, may be governed by a disclination unbinding-type mechanism [22–24], as proposed by the Kosterlitz-Thouless (KT) theory [25] (in fluids of hard ellipses, for which simulations exist [22,26,27], the nature of the transition seems to depend on the aspect ratio [27]). Mean-field theories, which cannot account for these effects since collective fluctuations and the dynamics of topological defects are not properly (or not at all) described, predict continuous transitions of the usual (mean-field) type [28–30]. However, the direct role played by dimensionality in two-dimensional mixtures may be of secondary importance as far as entropically driven *demixing* transitions are concerned, since local entropic effects associated with packing may completely preempt KT-type effects; in this sense, the mechanisms governing these systems could be intimately connected with those operating in the corresponding three-dimensional mixtures, which are described qualitatively correctly by mean-field theories of the density-functional type [1].

Of particular interest is the case of hard rectangular particles, which might exhibit a so-called tetratic phase (N_t) in the one-component fluid [30–34]. The tetratic phase possesses two equivalent directors pointing along mutually orthogonal directions; it exhibits a symmetry higher than that of the particles making up the fluid (see Fig. 1 for a rendition of typical particle configurations in the isotropic, tetratic, and uniaxial nematic phases in the mixture). The nature of the transition from the I to the N_t phases is unknown, but density-functional studies predict it to be of second order [18,30]. A recent bifurcation analysis [31], combined with further calculations, which include three-body correlations [34], have not been conclusive as to the absolute thermodynamic stability of the tetratic phase with respect to phases with spatial order, although preliminary computer simulations [32–34] seem to support the tetratic phase as an intermediate phase between the isotropic phase and the crystalline phase, at least for aspect ratios less than ~ 7 – 9 [34]. However, questions remain as to the maximum aspect ratio that can support tetratic order (for example, experiments on non-equilibrium-vibrated monolayers of granular particles [35] extend it up to ~ 12), the interplay between the N_t and

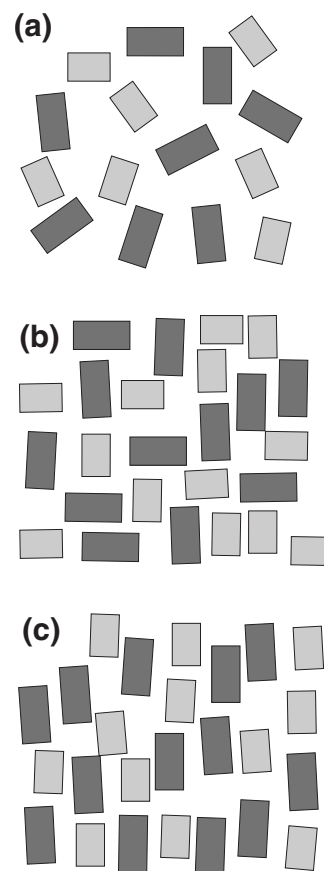


FIG. 1. Typical particle configurations of a binary mixture of hard rectangles in the (a) isotropic, (b) tetratic, and (c) uniaxial nematic phases.

the usual uniaxial nematic phase N_u (possessing only one director or alternatively two nonequivalent directors), or the role played by the nature of the crystalline tetratic phase (with an aperiodic solid being the most promising candidate [33]). Finally, recent work [36] has shown the ability of these particles to promote spatial order when confined between parallel one-dimensional plates, with potentially interesting applications as building blocks for self-assembly.

The role played by tetratic order in mixtures where one of the components consists of hard squares or rectangles, while the other may or may not promote this order, is the aim of the present paper. We investigate the phase behavior of mixtures of hard squares or hard rectangles with other particles of different geometry. The ability of hard rectangles to induce either short- or long-range tetratic order originates from the sharp corners of their shape (here we do not address the question on the existence of true long-range order of nematic correlations in these systems). Rectangles with low aspect ratio $\kappa=L/\sigma$ (with L their length and σ their breadth) may orient along either a particular direction or the orthogonal direction equally easily without hampering packing efficiency, and a tetratic phase results. For larger aspect ratios, hard rectangles stabilize into the usual uniaxial nematic. Hard-rod particles terminated by a semicircle (such as a discorrectangle) do not pack efficiently in a tetratic arrangement, and can only form one (uniaxial) nematic phase. When these

two types of particles, or when two types of hard rectangles—one exhibiting a tetratic phase which is not present in the other—mix together, the tetratic order induced by one component survives, at higher pressures, in some range of particle volume (area) fractions, with an extent that depends on the geometrical compatibility between species. Nematic demixing occurs, and the resulting phase diagrams show a rich variety of features, such as phase transitions of different order, triple, critical, tricritical, azeotropic, and critical end points.

A particular situation is when hard squares of different particle area are mixed. A consensus is now beginning to emerge that entropy-driven demixing in additive hard-sphere mixtures involves spatially nonuniform phases [3]. The current situation concerning mixtures of *parallel* (i.e., with frozen orientational degrees of freedom) hard cubes looks very similar [37]. Now, despite initial evidence based on simulation that no demixing occurs in a mixture of parallel hard squares on a lattice [38], supported by off-lattice density-functional calculations on the fluid phase [39], recent simulation work gives evidence for demixing involving an inhomogeneous phase [42]. In contrast, our calculations, which incorporate orientational degrees of freedom (though, admittedly, do not contemplate inhomogeneous phases), show demixing involving two fluid phases, at least one of which is oriented (with an island of instability in the phase diagram and sometimes with an associated upper critical point), when the size ratio is sufficiently large, while the completely isotropic mixture does not exhibit segregation. Clearly our results demand for additional computer simulations on the freely rotating hard-square model, which have not been reported yet.

After presenting a brief summary of the theoretical approach, which is a density-functional theory based on the SPT approximation, we present the results and conclude with a summary and some final remarks. The Appendix presents some details on the calculation of spinodal lines and tricritical points.

II. THEORY

Let us first briefly recall the theoretical model used and the approximations implemented. The model is based on the SPT approximation for two-dimensional binary mixtures, first applied in three dimensions by Cotter and Wacker [43]. The first extension to the two-dimensional case, a model of hard rectangles with restricted orientations [44], was later rederived for isotropic mixtures of general hard convex bodies [15]. Here we use the implementation of the SPT approximation for oriented mixtures derived, using the standard procedures in Ref. [18] to which the reader is referred for further details. Let us denote the free-energy density f in units of the thermal energy kT by Φ , i.e., $\Phi=f/kT$. The density functional for the corresponding excess (over ideal gas) quantity, $\Phi_{\text{exc}}[h_1, h_2]$, depends on the two orientational distribution functions $h_\nu(\phi)$ ($\nu=1, 2$) for the two components of the mixture, ϕ being the angle between the particle main axis and some reference direction in the plane, which is arbitrarily taken as the x axis. In SPT approximation it is written as [18]

$$\Phi_{\text{exc}}[h_1, h_2] = \rho \left\{ -\ln(1 - \eta) + \frac{\rho}{2(1 - \eta)} \sum_{\nu\tau} x_\nu x_\tau \langle \langle V_{\nu\tau}^{(0)} \rangle \rangle \right\}. \quad (1)$$

Here the subindices $\nu, \tau=1, 2$ refer to the two components of the mixture, $\rho=\rho_1+\rho_2$ is the total density, with ρ_ν the density of species ν , $\eta=\rho_1 v_1 + \rho_2 v_2$ is the total packing fraction, with v_ν the particle area for species ν , and the number fractions are defined as usual by $x_\nu=\rho_\nu/\rho$. Also, $V_{\nu\tau}^{(0)}(\phi)=V_{\nu\tau}(\phi)-v_\nu-v_\tau$ where $V_{\nu\tau}(\phi)$ is the angle-dependent, excluded volume between species ν and τ . The double angular average $\langle \langle V_{\nu\tau}^{(0)} \rangle \rangle$ is defined by

$$\langle \langle V_{\nu\tau}^{(0)} \rangle \rangle = \int_0^{2\pi} d\phi \int_0^{2\pi} d\phi' h_\nu(\phi) V_{\nu\tau}^{(0)}(\phi - \phi') h_\tau(\phi'). \quad (2)$$

The functions $V_{\nu\tau}(\phi)$ are analytical; their expressions were explicitly written in Ref. [18], except that corresponding to the cross interaction between rectangles and discorectangles [45].

Note that the one-component limit of Eq. (1) correctly reduces to the Onsager theory (where only the second virial coefficient is incorporated) as the density vanishes, since SPT recovers the exact second virial coefficient; however, in contrast to the three-dimensional case, the Onsager theory is not rigorously correct in the hard-needle limit in two dimensions, since three- and higher-order virial coefficients are *not* vanishingly small in this limit, some of them being even negative [46]. Therefore, higher-order contributions in density are only approximately reproduced by Eq. (1). SPT can be considered as a sophisticated Onsager theory in that spatial (not orientational, which are still included up to second order in density) correlations are somehow resumed into density-dependent terms. Alternative approaches, such as a two-dimensional version of the Parsons-Lee approach for three-dimensional hard rods, have the same structure and, for lack of a detailed performance analysis, can in principle be considered to be equivalent. The ideal contribution

$$\Phi_{\text{id}}[h_1, h_2] = \sum_{\nu} \rho_{\nu} \left(\ln \rho_{\nu} - 1 + \int_0^{2\pi} d\phi h_{\nu}(\phi) \ln [2\pi h_{\nu}(\phi)] \right) \quad (3)$$

is added to obtain the complete free energy-functional $\Phi[h_1, h_2]=\Phi_{\text{id}}[h_1, h_2]+\Phi_{\text{exc}}[h_1, h_2]$. Functional minimization of $\Phi[h_1, h_2]$ with respect to $h_\nu(\phi)$ gives the equilibrium configuration of the mixture. The pressure follows from the equation

$$\frac{p}{kT} = \frac{\rho}{1 - \eta} + \frac{\rho^2}{2(1 - \eta)^2} \sum_{\nu\tau} x_\nu x_\tau \langle \langle V_{\nu\tau}^{(0)} \rangle \rangle. \quad (4)$$

Instead of numerically solving the Euler-Lagrange equations associated with $\Phi[h_1, h_2]$, we follow common practice in our research group and tackle the direct minimization of the functional. Various strategies are possible [47]. In the present paper we choose to introduce a parametrized form

TABLE I. Possible values of the variational parameters $\Lambda^{(k)}$ and order parameters $q^{(k)}$ in the isotropic (I), uniaxial nematic (N_u), and tetratic (N_t) phases.

| Phase | $\Lambda^{(1)}$ | $\Lambda^{(2)}$ | $q^{(1)}$ | $q^{(2)}$ |
|-------------------------|-----------------|-----------------|-----------|-----------|
| Isotropic, I | 0 | 0 | 0 | 0 |
| Uniaxial nematic, N_u | >0 | ≥ 0 | >0 | >0 |
| Tetratic nematic, N_t | 0 | >0 | 0 | >0 |

for the orientational distribution functions, $h_\nu(\phi)$. To facilitate computations, these functions are simply parametrized as

$$h_\nu(\phi) = \frac{e^{\Lambda_\nu^{(1)} \cos 2\phi + \Lambda_\nu^{(2)} \cos 4\phi}}{\int_0^{2\pi} d\phi' e^{\Lambda_\nu^{(1)} \cos 2\phi' + \Lambda_\nu^{(2)} \cos 4\phi'}}. \quad (5)$$

The parameters $\Lambda_\nu^{(k)}$ take care of the two types of orientational symmetries, either uniaxial ($k=1$) or tetratic ($k=2$). Equivalently, two order parameters $q_\nu^{(k)}$ can be defined as

$$q_\nu^{(k)} = \int_0^{2\pi} d\phi h_\nu(\phi) \cos(2k\phi), \quad k=1,2, \quad (6)$$

which are proportional to the coefficients of a Fourier expansion of the functions $h_\nu(\phi)$ including the two lowest symmetries that a rectangular particle can generate. Table I summarizes the different phases with their associated values of the $\Lambda_\nu^{(k)}$ and $q_\nu^{(k)}$ parameters in a one-component phase. The equilibrium configurations of the mixtures are more conveniently obtained by minimizing the Gibbs free energy per particle $g=(p+f)/\rho$ with respect to the $\Lambda_\nu^{(k)}$ parameters at a fixed value of the pressure p and composition $x \equiv x_1$ (we will henceforth arbitrarily associate x with the number fraction of the component labeled as 1). Minimizations were performed using an efficient routine based on the Newton-Raphson method. Coexistence (binodal) lines were located by means of a standard common-tangent construction on $g(x)$, which guarantees equality of chemical potentials of both species in the two phases.

The use of the parametrization Eq. (5) obviously introduces an approximation over the exact calculation, and it would be of interest to know the amount of error introduced. As far as the calculation of bifurcation or spinodal lines of the various phase transitions is concerned, the parametrization has no impact, since first-order terms in $\Lambda_\nu^{(k)}$,

$$h_\nu(\phi) = \frac{1}{2\pi} (1 + \Lambda_\nu^{(1)} \cos 2\phi + \Lambda_\nu^{(2)} \cos 4\phi) + O(\Lambda_\nu^{(k)})^2, \quad (7)$$

which appear as quadratic terms in the free energy, are treated exactly. However, binodal lines and tricritical points are affected by the parametrization, since their location depends on higher-order terms in $\Lambda^{(k)}$. We have checked the parametrization in two ways: first, some selected calculations have been performed using an additional cosine term, $\cos 6\phi$

($\cos 8\phi$), in the parametrization for the uniaxial (tetratic) nematic phase; the differences found, at the level of coexistence lines, were found immaterial. Second, tricritical points have been evaluated exactly by computing the exact fourth-order terms (involving the above cosine terms depending on the symmetry of the phase). In all cases the differences with respect to the calculations using Eq. (5) have been found to be of minor importance. The analysis is presented in the Appendix, which contains quantitative details on this issue.

III. RESULTS

Results are presented, in the form of pressure-composition phase diagrams, in Figs. 2–9. We divide the presentation by first showing results for different mixtures containing squares and disks, followed by mixtures of hard rods (rectangles and discorectangles). In the following we will generally use the following acronyms for the different particles: HS (hard squares), HD (hard disks), HR (hard rectangles), and HDR (hard discorectangles).

A. Mixtures of hard squares

The fluid of freely rotating hard squares has been studied by Monte Carlo simulations [32], with indications that a tetratic phase might be stable prior to crystallization. On the other hand, mixtures of hard squares have been analyzed by computer simulations [38,42] and density-functional theory [39] in the approximation of perfect orientational order. Indications that there is no demixing in this system [27,38] were later challenged by evidence for a spinodal line from Monte Carlo simulation [42]; the demixing transition involves a fluid phase and a phase with big squares in close-packed aggregates. Since orientational disorder may be important for these mixtures, we believe it is of interest to address this problem with the SPT approximation, where orientational disorder is allowed (obviously our approach can only search for demixing behavior involving fluid, either isotropic or tetratic, phases).

The results shown in Fig. 2 correspond to a mixture of freely rotating squares with size ratio 1:10, and have been gathered in a pressure-composition phase diagram, with label 1 assigned to the larger particles. According to SPT theory, the fluids of the unmixed (one-component) species both exhibit corresponding second-order I - N_t phase transitions at reduced pressure $pv/kT \approx 0.52$ (here v is the particle proper area). Note that, for squares, a uniaxial nematic phase is not possible by construction. For the mixture, the only possible (fluid) phases are also the I and N_t phases. Remarkably, the mixture exhibits segregation between two tetratic phases with different area fractions occupied by the two components. The region of demixing is a closed loop bounded above (below) by an upper (lower) critical point (in fact, since the I - N_t spinodal line crosses the demixing region—see inset showing schematic topology—segregation mostly proceeds between I and N_t phases). Since mixtures of perfectly parallel hard squares do not demix it is surprising that, in this mixture, orientational disorder induces demixing.

Closed loops of immiscibility have been predicted in mixtures of hard rods in the Onsager approximation [7,8] (see,

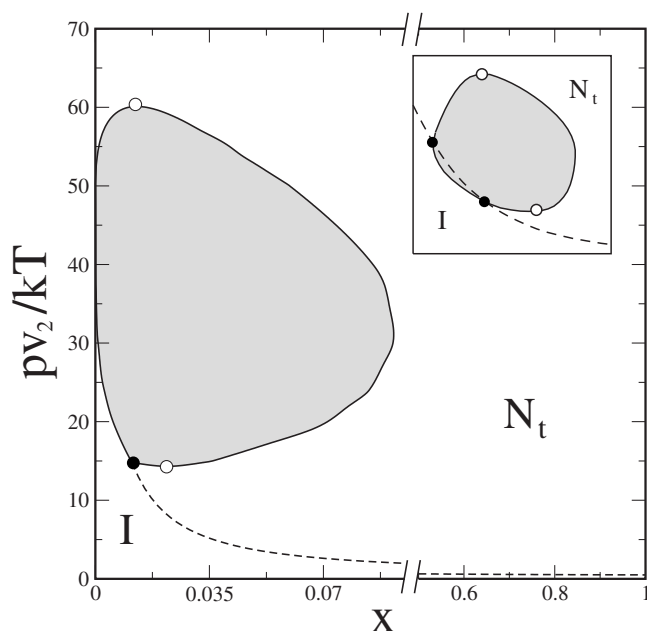


FIG. 2. Phase diagram of a hard-square ($L_\nu = \sigma_\nu$ for $\nu=1,2$) mixture with $L_1/L_2=10$ in the scaled-pressure pv_2/kT vs composition $x=x_1$ plane. Open circles: critical points. Filled circles: critical end points. The inset is a qualitative scheme depicting the relative locations of the $I-N_t$ spinodal and the region of demixing. The two-phase region is indicated by the gray area. Note that the scale of the composition (horizontal) axis is discontinuous.

however, Ref. [48]), and also in fluids of parallel hard rods [49], both in three dimensions. Our calculations show that they are also a property of some two-dimensional mixtures. In our case demixing occurs at fairly low values of composition; this is easy to explain since we expect segregation to take place when the volume fraction of both components are approximately equal, $\eta_1 \approx \eta_2$, which implies that segregation will occur for $x \sim v_2/v_1 = 10^{-2}$. As the size ratio of the squares decreases, the island of immiscibility diminishes, and we are eventually left with a second-order $I-N_t$ transition in the whole composition interval. The demixing island disappears when the size ratio is equal to 1:4 (see the Appendix).

The mechanism underlying N_t-N_t demixing is different for the upper and lower parts of the demixing island. As is well known, demixing and ordering phenomena in mixtures of hard anisotropic particles result from the competition of entropies of different origin: mixing, orientational, and excluded-volume entropies. In the transition from the isotropic to the nematic phase the last two terms compete. In mixtures, the excluded-volume entropy has contributions from the two species and from the unlike-particle interactions. The mechanism explaining the lower N_t-N_t segregation phenomena in Fig. 2 is the classical one: the balance between mixing entropy and the excluded-volume term of unlike species, which counterbalances the tendency toward mixing of the former. However, the upper N_t-N_t segregation region has a different origin, since here orientational entropy plays a role. This might have been suspected *a priori*, since in the limit of perfect order (parallel squares) no demixing occurs. At sufficiently high pressures in the freely rotating fluid, suffi-

ciently near the close-packed limit, the orientational order is almost saturated and can no longer compete with the other terms, so that no demixing is expected. As pressure is reduced, orientational entropy begins to play a role and in fact, the contribution from the small squares is the driving force toward demixing.

For the size ratio shown (1:10), two critical end points, indicated in the figure by filled circles, appear in the phase diagram, defined by the points where the $I-N_t$ spinodal line crosses the demixing region. Note that, on general grounds, a critical end point is defined in a situation where two phases coexist, one of them being a critical phase. A critical end point can be defined by a coexistence condition (common-tangent construction in our computational scheme) plus a condition for criticality (loss of convexity of the Gibbs free energy of one of the phases). However, this point cannot be obtained analytically (contrary to the tricritical points) and, similar to the binodal lines, has to be calculated numerically. In our case, the location of these points, given by $x^{(1)*} = 0.012$, $p^{(1)*}v_2/kT = 13.86$, and $x^{(2)*} = 8 \times 10^{-5}$, $p^{(2)*}v_2/kT = 49.38$, can be approximated from the set of candidates to tricritical points obtained by means of a bifurcation analysis (here and in what follows, numerical values for the location of tricritical points should be understood to result from rigorous bifurcation analysis of the free-energy functional, and may in some cases be at variance with those obtained from the variational minimization, on which all the phase diagrams presented are based; see the Appendix for details on the bifurcation analysis). As the size ratio is diminished, first the upper critical point disappears, and the upper critical end point becomes a tricritical point; then the lower critical end point becomes a tricritical point, and the lower critical point also disappears, leaving two tricritical points before the whole demixing region vanishes. The lower critical point always stays within the N_t region (i.e., no $I-I$ demixing is observed).

Demixing in this mixture is therefore associated with a symmetry-breaking phase, the tetratic phase. There are strong arguments [15] disallowing demixing in the I phase (within the context of the SPT approach). This would not necessarily imply that demixing is completely ruled out in the rotationally symmetric I phase of hard-square mixtures or mixtures of particles with different geometries, but a more sophisticated theory, incorporating exact higher-order virial coefficients (which are known to be important for two-dimensional hard convex bodies), would be necessary to settle this point.

B. Mixtures containing squares and disks

Figure 3 shows the phase diagram corresponding to a mixture of hard disks and squares (the diameter of the former being equal to the side length of the latter). Here only one of the components (the squares) has tetratic order. By choosing the particle areas of both species to be approximately equal (the ratio being ≈ 0.79) we focus on the role of particle geometry. In this mixture we find that the N_t phase exhibited by the pure system of squares survives up to a maximum concentration of disks of $\sim 50\%$ (this corresponds to an area

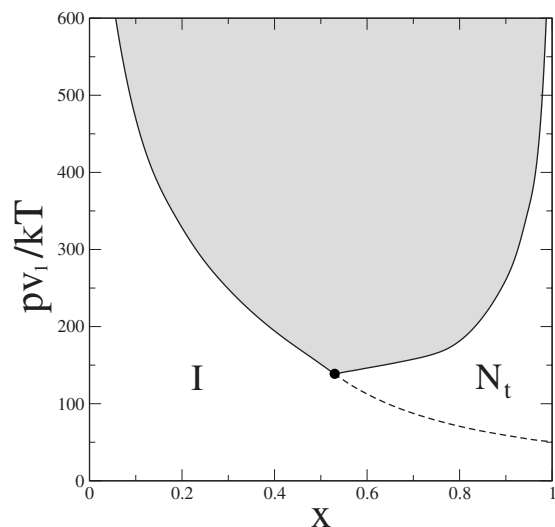


FIG. 3. Phase diagram for a HS/HD mixture in the scaled-pressure pv_1/kT vs composition $x=x_1$ plane, with $v_1=L_1\sigma_1$ the volume of the squares. The side length of the squares, $L_1=\sigma_1$, is chosen to be the same as the diameter of the disks, σ_2 . The filled circle indicates a tricritical point. The two-phase region is indicated by the gray area.

ratio approximately equal to 0.79). Complete demixing occurs at high pressure, while the $I-N_t$ transition becomes of second order below a tricritical point, located at $x=0.57$, $pv_1/kT=131.95$ (see the Appendix). Fractionation becomes stronger as pressure is increased, since excluded-volume considerations are increasingly important in this limit: geometrical mismatch (given by the unlike disk-square interaction) grossly counterbalances mixing entropy, inducing strong segregation.

C. Mixtures of rectangles and discorectangles

Hard rectangles have been predicted to exhibit a phase with tetratic order when their aspect ratio is sufficiently low [30–34]. Tetratic order is enhanced as the aspect ratio of the rectangles is decreased. However, there is some uncertainty as to the critical value of κ beyond which the tetratic phase is no longer possible; the SPT approach indicates that for $\kappa < 2.21$ the stable nematic phase is the tetratic nematic [50] (as mentioned in the introduction, computer simulations indicate that this value may be much larger, in the range ~ 7 – 9). In contrast, a fluid of hard discorectangles can only support a uniaxial nematic phase [23].

In previous work [18] we analyzed possible demixing scenarios of mixtures of hard rectangles (HR) and mixtures of hard discorectangles (HDR), using the same SPT theory. In this section we further investigate this problem by considering a wider range of mixtures, in particular, *crossed* mixtures (i.e., mixtures consisting of HR and HDR particles); the effect of particle geometry is an aspect that can be assessed in a very direct way by analyzing crossed mixtures, as well as the role played by the tetratic phase against the standard uniaxial nematic phase when particles of different geometries are mixed. Results will be presented by means of phase

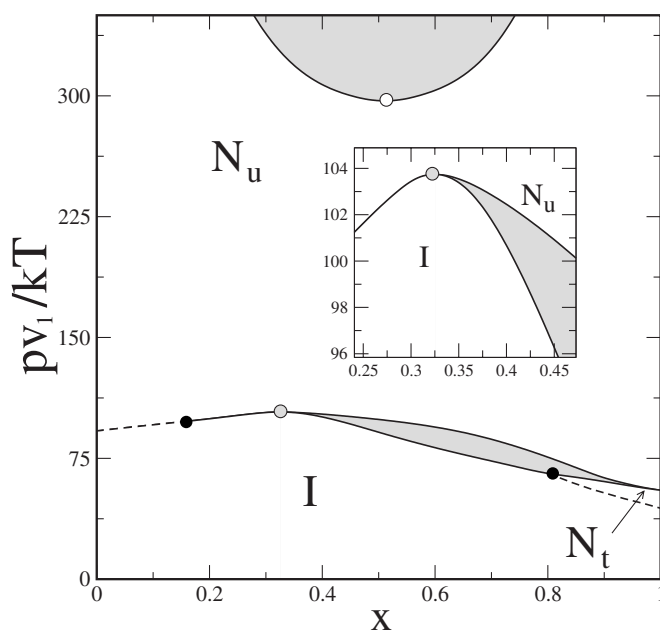


FIG. 4. Phase diagram for a HR/HDR mixture in the scaled-pressure pv_1/kT vs composition x plane. The two components have the same aspect ratio [$\kappa_1=L_1/\sigma_1=2$ for the rectangles and $\kappa_2=(L_2+\sigma_2)/\sigma_2=2$ for the discorectangles], and the same particle area. The open circle indicates the critical point, the shaded circle denotes an azeotropic point, while the filled circles indicate tricritical and critical-end points. Two-phase regions are indicated by gray areas.

diagrams including, not only spinodal lines, but also binodal lines when present.

In the following we first consider mixtures of hard rods, one of which can be stabilized into a tetratic phase (i.e., HR particles with aspect ratio $\kappa < 2.21$) while the other cannot (i.e., either HR particles with $\kappa > 2.21$, or HDR particles). We intend to understand how the tetratic phase is destabilized by the geometrical mismatch of the particles.

The first mixture that we consider is a mixture of HR and HDR particles, both with $\kappa=2$ [in the latter case the aspect ratio parameter is defined as $\kappa=(L+\sigma)/\sigma$]. Also, the same particle areas have been chosen for both types of particles, in an attempt to single out features of phase behavior mainly driven by differences in particle geometry. The resulting phase diagram is depicted in Fig. 4. At high pressure a demixing region occurs between two uniaxial nematic phases (i.e., there is N_u-N_u demixing), bounded by a lower critical point. Fractionation becomes stronger as pressure increases, an effect ultimately associated with the slight difference in particle geometry, which penalizes the mixed state due to unfavorable packing between dissimilar particles; this arises from the circular caps of the HDR particles. At lower pressure there is a transition between the isotropic and the uniaxial nematic phases, which occurs via a first-order phase transition with small fractionation. The phase diagram is of the azeotropic type: an azeotropic point (no fractionation) appears at $x \approx 0.32$, with an associated (small) pressure range where the N_u phase is reentrant. Since the HR component of the mixture possesses a stable tetratic phase, an island of

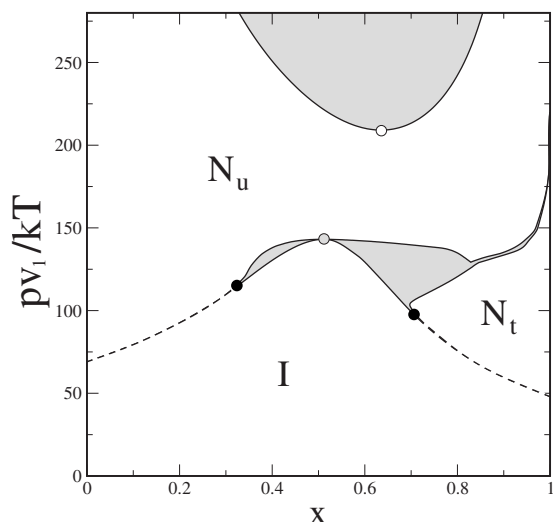


FIG. 5. Phase diagram for a HR/HDR mixture in the scaled-pressure pv_1/kT vs composition x plane. Values of the parameters are $\kappa_1=1.5$, $\sigma_1=1$ for the rectangles and $\kappa_2=2$ and the same particle area as a rectangle of aspect ratio equal to 2 and unit breadth for the discorectangles. The open circle indicates the critical point, the shaded circle denotes an azeotropic point, while the filled circles indicate tricritical points. Two-phase regions are indicated by the gray areas.

tetratic order exists for high values of x , separated from the isotropic phase via a second-order phase transition and from the uniaxial nematic via a first-order transition (of course this is also the case for the pure HR fluid, $x=1$). The island of N_t stability is very small; for a HR fluid with $\kappa=2$, the range of pressures where the tetratic phase is stable is small [31] but, in addition, tetratic order is easily destroyed when adding to the mixture particles that do not conform with tetratic symmetry.

Next we consider two different mixtures that represent slight variations with respect to the previous mixture. In Fig. 5 we analyze a HR/HDR mixture, where the HR component has been shortened to an aspect ratio of $\kappa_1=1.5$, keeping the breadth to the same value, while the HDR component still has $\kappa_2=2$ but the particle area is made equal to that of the HR particle of the previous mixture (while at the same time reducing its particle area by 25%) with the aim of increasing the strength of tetratic ordering. Since the tetratic phase of the one-component HR fluid is much more stable, the tetratic phase in the mixture stabilizes into a larger range of compositions. The diagram is topologically equivalent to that in Fig. 4, except that the critical end point in the $I-N_t$ spinodal line now becomes a tricritical point, and there appears a (new) $I-N_u-N_t$ triple point.

Nontrivial changes are obtained if the mixture of Fig. 4 is changed by shortening the HDR particle down to an aspect ratio of $\kappa_2=1.5$ while the particle area is made equal to that of a HR particle of aspect ratio 1.5 and unit breadth; as a result, the nematic phase of the one-component HDR fluid appears at a much higher pressure. The phase diagram is presented in Fig. 6. This phase diagram can be regarded as a

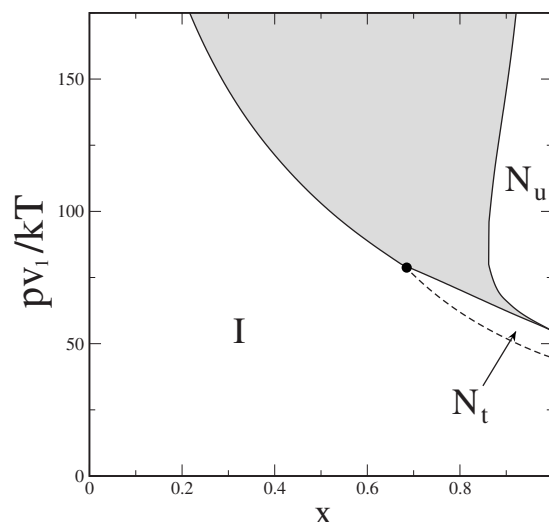


FIG. 6. Phase diagram for a HR/HDR mixture in the scaled-pressure pv_1/kT vs composition x plane. Values of the parameters are $\kappa_1=2$, $\sigma_1=1$ for the rectangles and $\kappa_2=1.5$ and the same particle area as the rectangle of aspect ratio equal to 1.5 and the unit breadth for the discorectangles. The filled circle indicates critical end points. The two-phase region is indicated by the gray area.

continuation of that in Fig. 4 where the N_u-N_u demixing region and the $I-N_u$ coexistence have collapsed into a single demixing region. The $I-N_t$ phase stability region now increases, as a result of the HDR particle having a lower proper area.

D. Mixtures of rectangles

Finally, we consider mixtures of HR particles. Here the breadth of all particles will be taken to be unity, and we change the length or, equivalently, the aspect ratio. Three cases are considered: (i) $\kappa_1=5$, $\kappa_2=10$, so that none of the components exhibits tetratic symmetry; (ii) $\kappa_1=2$, $\kappa_2=1.5$, with both species having tetratic phases; and (iii) κ_1 in the range 4.0–5.0, $\kappa_2=2$, so that only the second species can stabilize into a tetratic phase. This cases are shown in Figs. 7–9, respectively.

In mixture (i) no tetratic phase appears (Fig. 7). There is N_u-N_u demixing at high pressure. The $I-N_u$ transition is of first order, but becomes of second order at a tricritical point (see inset), located at $x=0.35$, $pv_1/kT=4.07$ (see the Appendix).

The aspect ratios of the two components of mixture (ii), $\kappa_1=2$ and $\kappa_2=1.5$, were chosen such that both possess a stable tetratic phase. This requires their values to be very similar; therefore, no demixing occurs (Fig. 8), and a relatively featureless phase diagram results.

Finally, in mixture (iii), the shorter component exhibits a tetratic phase that propagates from the $x=0$ axis into finite values of composition when the longer component is added; however, due to the considerable difference in lengths between the two species, the N_t phase does not survive very much as a function of composition; in fact, the region of tetratic stability can hardly be seen in the phase diagram, Fig.

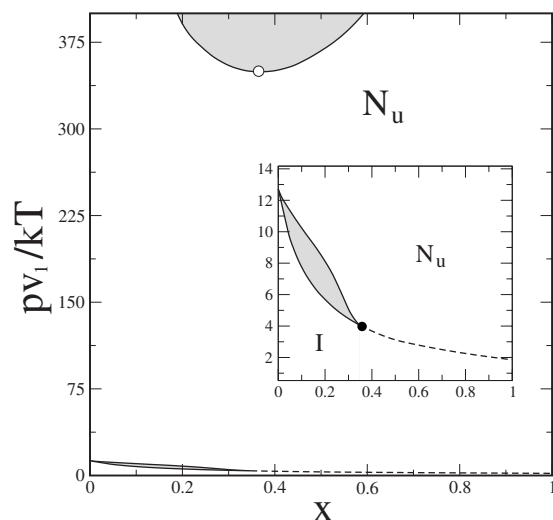


FIG. 7. Phase diagram for a HR/HR mixture in the scaled-pressure pv_1/kT vs composition x plane. Particle breadths are set to the same value, while aspect ratios are $\kappa_1=10$ and $\kappa_2=5$. Open circle: critical point. Filled circle: tricritical point. Two-phase regions are indicated by the gray areas.

9. At high pressure there is a large demixing region which, as the particle aspect ratio of the first component is increased (from 4.0 to 5.0), expands considerably. Again demixing is due to unfavorable excluded-volume interactions between unlike species. In general, the phase diagram varies considerably even for very slight variations in particle shape of the first species. For $\kappa_1=4.0$ and 4.6, a separate region associated with the first-order $I-N_u$ transition appears at low pressures; in some cases (cf. the case $\kappa_1=4.6$) reentrant behavior in the nematic phase (stronger than in three-dimensional hard-rod mixtures-see, e.g., Ref. [5]), is found. Also, for the case $\kappa_1=4.6$ an *upper* critical point associated with N_u-N_u

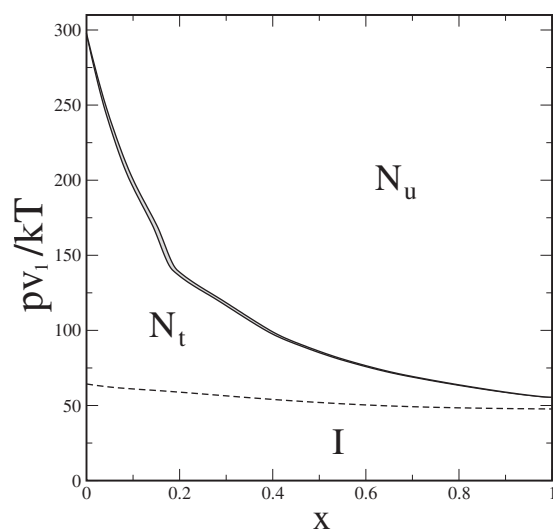


FIG. 8. Phase diagram for a HR/HR mixture in the scaled-pressure pv_1/kT vs composition x plane. Particles have the same breadth, with $\kappa_1=2$ and $\kappa_2=1.5$. The two-phase region is indicated by the gray area.

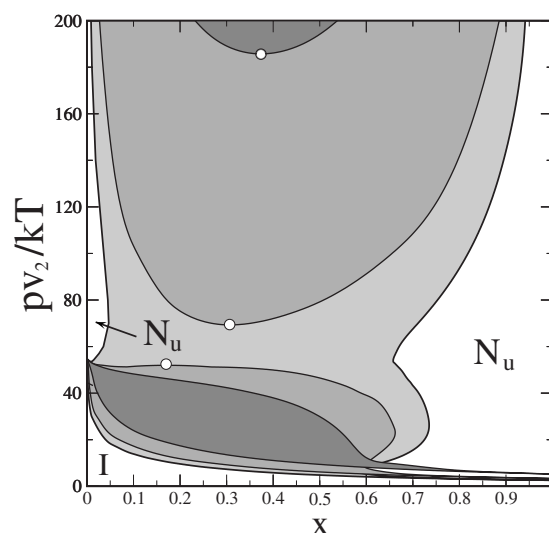


FIG. 9. Phase diagram for a HR/HR mixture in the scaled-pressure pv_2/kT vs composition x plane. All rectangles are taken to have the same breadth, and $\kappa_2=2$. The first component has $\kappa_1=4.0, 4.6$, and 5.0, corresponding to two-phase regions in lighter gray in the graph.

demixing can be seen. This feature has been seen in three-dimensional mixtures of thin and thick hard rods of the same length; in our two-dimensional mixture the particle thickness is the same, and it is particle length that is different. Therefore, in some range of parameters two N_u-N_u coexistence regions can be found, with upper and lower critical points. These two regions merge as κ_1 increases, giving rise to a very large demixing region.

IV. DISCUSSION AND CONCLUDING REMARKS

To conclude, we have analyzed the phase behavior of mixtures of two-dimensional hard rods, using the scaled-particle theory approximation. We have particularly concentrated on mixtures containing hard rectangles as one of the components, with the other being a hard discorectangle, which we have called *crossed* mixtures. The geometry of hard rectangles allows for a tetratic phase to be stabilized; addition of a second component, which does not support this symmetry, obviously tends to destroy tetratic order but, when the particle areas of both components are not very dissimilar and the pure fluid of hard rectangles strongly stabilizes the tetratic phase (i.e., when their aspect ratio is relatively low), tetratic order may survive even for large area fractions of the non-tetratic-forming component. The case of a mixture of hard rectangles, one with tetratic order and the other without, shows the same trends.

As a special case we have also considered mixtures of hard squares, and found that these mixtures do exhibit nematic demixing, contrary to the case where rotational degrees of freedom are frozen; in the latter case the mixture never segregates into two fluid phases (though simulations seem to point to segregation between fluid and nonuniform phases), while in the former there is a critical size ratio (1:4) above

which there is segregation. This is a remarkable case where orientational *disorder* induces entropy-driven demixing (i.e., *mixing order*). Inclusion of nonuniform phases in our theoretical analysis would certainly be interesting and is left for future work. Growing evidence indicates that demixing in additive hard-core mixtures always involves at least one inhomogeneous phase. An interesting possibility is that freely rotating hard-core mixtures (which can be viewed as a special case of nonadditive mixture) may in some cases segregate into two fluid phases, provided nematic phases are involved; it could be that some type of symmetry breaking, either positional or orientational, is required for demixing to occur.

In general, phase diagrams of two-dimensional hard-rod particles closely resemble those of three-dimensional mixtures, save the fact that the isotropic-nematic transition in two dimensions may be (and actually is in most cases) of second order, which adds an element of complexity to the corresponding phase diagrams. Nematic-nematic demixing generally occurs in these systems and, for sufficiently large size ratios between the components, demixing competes with the isotropic-nematic (either uniaxial or tetratic) transition. Entropic effects due to balance between excluded-volume interactions of like and unlike components and mixing entropy produce strong fractionation. These effects probably counteract collective fluctuations leading to KT-type behavior; for example, within our mean-field density-functional treatment, the continuous isotropic-nematic transition of the one-component fluid generally continues as a critical transition in the mixture, but sooner or later, beyond some value of particle composition, a demixing (first-order) transition is met via a tricritical point or otherwise (critical end point). However, the true nature of the isotropic-nematic transition in these mixtures, and of the uniaxial and tetratic nematic phases themselves (i.e., whether they possess true or quasi-long-range order) is an issue that should be investigated by means of detailed computer simulations and possibly also by experiments on vibrated monolayers.

In this work we have not considered spatially ordered phases, such as smectic, columnar, or crystalline. Certainly some of these phases will appear at some pressure, and probably some of the phase behavior shown for the mixtures considered will be preempted by these phases. More sophisticated density-functional treatments are required to assess this point; some proposals have already been done for one-component two-dimensional hard-rod systems [31], but even the consequences of these approaches have not been explored yet; this will be the subject of future work [51].

ACKNOWLEDGMENTS

Y.M.-R. was supported by a Ramón y Cajal research contract. This work is part of the research projects MOSAICO, Grants No. FIS2005-05243-C02-01 and No. FIS2004-05035-C03-02 of the Ministerio de Educación y Ciencia (Spain), and Grant No. S-0505/ESP-0299 of Comunidad Autónoma de Madrid (Spain).

APPENDIX: BIFURCATION ANALYSIS

In Ref. [18] two of us carried out a bifurcation analysis to study the nature of phase transitions in two-dimensional

hard-rod fluid mixtures and to calculate the location of the tricritical points present in their phase diagrams. We refer the reader to this work for details on the calculations. For the sake of completeness, a brief summary of the main ingredients of the bifurcation analysis is presented here.

The Fourier series representation of the orientational distribution functions of the two different species, labeled as $\nu=1,2$, is

$$h_\nu(\phi) = \frac{1}{2\pi} \left[1 + \sum_{k \geq 1}^{\infty} h_k^{(\nu)} \cos(2k\phi) \right]. \quad (\text{A1})$$

After inserting these expressions in the free energy per particle $\varphi = \Phi/\rho$ and expanding in Taylor series with respect to the Fourier amplitudes $h_k^{(\nu)}$, we obtain a Landau expansion for $\Delta\varphi = \varphi_N - \varphi_I$, the free-energy difference between the orientationally ordered and isotropic phases, in terms of these amplitudes. Further, minimizing $\Delta\varphi(\{h_k^{(\nu)}\})$ with respect to all amplitudes except one (here chosen as $h_i \equiv h_i^{(1)}$, with $i=1,2$ for uniaxial and tetratic nematic phases, respectively), and substituting the result back in $\Delta\varphi$, keeping terms up to fourth order, we obtain the expression

$$\Delta\varphi = Ah_i^2 + Bh_i^4. \quad (\text{A2})$$

The coefficients $A(x, \eta)$ and $B(x, \eta)$ are both functions of the composition $x \equiv x_1$ and packing fraction η . The spinodal curve of the transition between the isotropic and nematic (uniaxial or tetratic) phases can be calculated as $A(x, \eta^*)=0$, which defines the packing fraction $\eta^*(x)$ as a function of the composition.

It can be shown [18] that the instability region of the mixture with respect to composition and volume fluctuations defines a region in the plane (κ_1, x) , at fixed κ_2 , bounded by curves calculated as the roots of the function T_N^* , defined by

$$T_N^* = T_I^* - \frac{1}{2B^*} \left[\frac{\partial}{\partial y} \left(y^2 \frac{\partial \varphi_I}{\partial y} \right)^* (A_x^*)^2 + \left(\frac{\partial^2 \varphi_I}{\partial x^2} \right)^* (y^* A_y^*)^2 - 2 \left(\frac{\partial^2 \varphi_I}{\partial x \partial y} \right)^* (y^*)^2 A_x^* A_y^* \right], \quad (\text{A3})$$

where

$$T_I = \frac{\partial}{\partial y} \left(y^2 \frac{\partial \varphi_I}{\partial y} \right) \left(\frac{\partial^2 \varphi_I}{\partial x^2} \right) - \left(y \frac{\partial^2 \varphi_I}{\partial x \partial y} \right)^2. \quad (\text{A4})$$

Here $y = \rho/(1-\eta)$, and the asterisk over any function of y means that this function is to be evaluated at y^* , its bifurcation value (note the different definition of y with respect to the one used in Ref. [18]; both coincide when $\nu_\nu=1$, the constraint used in Ref. [18]). Finally, A_x^* and A_y^* are the partial derivatives of A with respect to x and y , respectively, both evaluated at y^* .

1. Mixtures of hard squares

The packing fraction of the spinodal line obtained as the solution of $A(x, \eta^*)=0$ is a constant, independent of x , and is equal to $\eta^* = [1+8/(15\pi)]^{-1}$. Further, the $I-N_i$ tricritical points can be calculated as the roots of

$$T_{N_t}^* = \frac{16}{x_1 x_2} \left\{ 1 - \frac{2}{11} s_3^2 \left[1 + s_2^2 + 15 \frac{(s_2 - s_1)^2}{1 + s_1^2} \right] \right\}, \quad (\text{A5})$$

with

$$s_i = \sqrt{\frac{\langle \sigma^{2i} \rangle}{\langle \sigma^i \rangle^2}} - 1, \quad i = 1, 2, \quad s_3 = \sqrt{\frac{11 \langle \sigma^2 \rangle^3}{16 \langle \sigma^4 \rangle \langle \sigma^2 \rangle - 5 \langle \sigma^3 \rangle^2}}, \quad (\text{A6})$$

where we defined $\langle u^n \rangle = \sum_i x_i u_i^n$. Introducing the new variable $\xi = x_2 v_2 / \langle v \rangle$, and after some lengthy but straightforward calculations, we arrive at

$$T_{N_t}^* = \frac{16}{x_1 x_2} \frac{[25z^2 + (34 - 16r)z + 9]}{[11 + z(16r + 6 - 5z)]}, \quad (\text{A7})$$

where the new variable $z = (r-1)\xi$ was introduced, and we defined $r = \sigma_1 / \sigma_2$. The quadratic equation of z given in the numerator of Eq. (A7) has the following roots:

$$\xi_{1,2} = \frac{1}{25(r-1)} [8r - 17 \pm 4\sqrt{(r-4)(4r-1)}]. \quad (\text{A8})$$

We can see from this expression that demixing can only occur for $r > 4$. The pressure at the tricritical point can be calculated using the value of the roots found above, resulting in

$$\frac{p^* \sigma_1^2}{kT} = \frac{15\pi}{8r^2} \left[r^2 - (r^2 - 1)\xi + \frac{15}{2} [r - (r-1)\xi]^2 \right]. \quad (\text{A9})$$

For $r=10$ we find

$$\xi_{1,2} = \frac{1}{75} (21 \pm 4\sqrt{26}), \quad (\text{A10})$$

with the approximate values $\xi_1 \approx 0.5519$ and $\xi_2 \approx 0.0081$. Using $x_2 = \xi / [r^2 - (r^2 - 1)\xi]$, we find $x_2^{(1)*} \approx 0.0122$ and $x_2^{(2)*} \approx 8.12 \times 10^{-5}$, while the values for the pressures are $p^{(1)*} \sigma_1^2 / kT \approx 13.8603$ and $p^{(2)*} \sigma_1^2 / kT \approx 49.3842$.

In Fig. 10 are shown the mixed and demixed states of the hard-square mixture in the ξ - r^{-1} plane, as obtained from the roots in Eq. (A8). We have checked that this is indeed the scenario for values of r not too much larger than its critical value $r^* = 4$, i.e., the I - N_t transition changes from second (first) to first (second) order above (below) the lower (upper) tricritical point. As we have already shown, the phase diagram for $r=10$ has two critical points, but the tricritical points are located close to the critical end points (see Fig. 2).

2. Mixtures of hard squares and hard disks

The solution to the equation $A(x, \eta^*) = 0$ gives us the following expression for the isotropic-tetrahedral spinodal curve:

$$\eta^* = \left[1 + \frac{8x\sigma_1^2}{15\pi \langle v \rangle} \right]^{-1}, \quad (\text{A11})$$

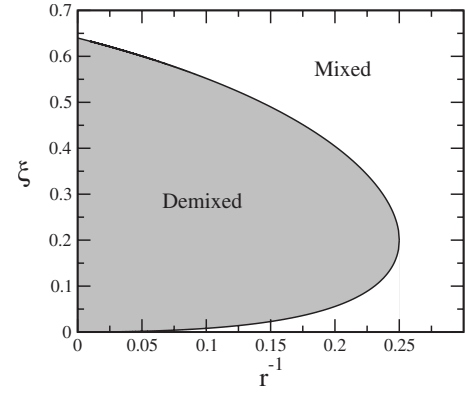


FIG. 10. The mixed and demixed states that follow from the solution to $T_{N_t}^* = 0$, with $T_{N_t}^*$ given by Eq. (A7).

while the solution to $T_{N_t}^* = 0$ can be found also analytically as

$$x^* = \left[1 + \frac{16}{35} \left(\frac{4\sigma_1}{\pi\sigma_2} \right)^2 \right]^{-1}. \quad (\text{A12})$$

Finally, the pressure at the tricritical point can be calculated as

$$\frac{p^* \sigma_1^2}{kT} = \frac{15\pi}{8x^*} \left\{ 1 + \frac{15}{2x^* \sigma_1^2} \left[\frac{\pi\sigma_2}{4} + \left(\sigma_1 - \frac{\pi\sigma_2}{4} \right) x^* \right]^2 \right\}. \quad (\text{A13})$$

For $\sigma_1 = \sigma_2 = 1$ we find $(x^*, p^* v_1 / kT) \approx (0.5744, 131.9459)$. The value for the composition calculated from the minimization is about 0.53 (see Fig. 3). This difference is due to the parametrization used. One should include, in the exponential parametrization of the orientational distribution functions, terms such as $\Lambda_v^{(2)} \cos 4\phi + \Lambda_v^{(4)} \cos 8\phi$ to properly take into account the tetrahedral symmetry about the tricritical point.

3. Mixtures of hard rectangles

For mixtures of hard rectangles the isotropic-uniaxial nematic spinodal calculated as the solution to $A(x, \eta^*) = 0$ gives

$$\eta^* = \left[1 + \frac{2}{3\pi} \frac{\langle (L - \sigma)^2 \rangle}{\langle v \rangle} \right]^{-1}. \quad (\text{A14})$$

The value of the pressure at bifurcation is

$$\frac{p^* v_1}{kT} = y^* \left[1 + \frac{3}{2} \frac{\langle (L + \sigma)^2 \rangle}{\langle (L - \sigma)^2 \rangle} \right]. \quad (\text{A15})$$

Solving $T_N(x, \eta^*) = 0$ numerically with respect to x for a particular mixture with $(L_1 = 10, \sigma_1 = 1)$ and $(L_2 = 5, \sigma_2 = 1)$, we find a value of $x^* \approx 0.3472$, which defines the location of the tricritical point. The packing fraction and the pressure at this point are $\eta^* \approx 0.4515$ and $p^* v_1 / kT \approx 4.0659$, respectively.

- [1] G. J. Vroege and H. N. W. Lekkerkerker, *Rep. Prog. Phys.* **55**, 1241 (1992).
- [2] T. Itou and A. Teramoto, *Macromolecules* **17**, 1419 (1984); *Polym. J. (Tokyo, Jpn.)* **16**, 779 (1984); P. Buining and H. N. W. Lekkerkerker, *J. Phys. Chem.* **97**, 11510 (1993); G. Nounesis, S. Kumar, S. Pfeiffer, R. Shashidhar, and C. W. Garland, *Phys. Rev. Lett.* **73**, 565 (1994); F. M. van der Kooij and H. N. W. Lekkerkerker, *ibid.* **84**, 781 (2000); K. R. Purdy, S. Varga, A. Galindo, G. Jackson, and S. Fraden, *ibid.* **94**, 057801 (2005).
- [3] J. L. Lebowitz and J. S. Rowlinson, *J. Chem. Phys.* **41**, 133 (1964); G. A. Mansoori, N. F. Carnahan, K. E. Starling, and T. W. Leland, *ibid.* **54**, 1523 (1971); T. Biben and J.-P. Hansen, *Phys. Rev. Lett.* **66**, 2215 (1991); H. N. W. Lekkerkerker and A. Stroobants, *Physica A* **195**, 387 (1993); M. Dijkstra, R. van Roij, and R. Evans, *Phys. Rev. Lett.* **82**, 117 (1999).
- [4] P. J. Flory and A. Abe, *Macromolecules* **11**, 1119 (1978).
- [5] H. N. W. Lekkerkerker, Ph. Coulon, R. van der Haegen, and R. Deblieck, *J. Chem. Phys.* **80**, 3427 (1984).
- [6] T. Odijk and H. N. W. Lekkerkerker, *J. Phys. Chem.* **89**, 2090 (1985).
- [7] T. M. Birshtein, B. I. Kolegov, and V. A. Pryamitsyn, *Polym. Sci. U.S.S.R.* **30**, 316 (1988).
- [8] G. J. Vroege and H. N. W. Lekkerkerker, *J. Phys. Chem.* **97**, 3601 (1993).
- [9] R. van Roij and B. Mulder, *Phys. Rev. E* **54**, 6430 (1996).
- [10] S. Varga, K. Purdy, A. Galindo, S. Fraden, and G. Jackson, *Phys. Rev. E* **72**, 051704 (2005).
- [11] T. Koda and H. Kimura, *J. Phys. Soc. Jpn.* **63**, 984 (1994).
- [12] G. Cinacchi, L. Mederos, and E. Velasco, *J. Chem. Phys.* **121**, 3854 (2004).
- [13] Y. Martínez-Ratón, E. Velasco, and L. Mederos, *J. Chem. Phys.* **123**, 104906 (2005).
- [14] G. Cinacchi, Y. Martínez-Ratón, L. Mederos, and E. Velasco, *J. Chem. Phys.* **124**, 234904 (2006).
- [15] J. Talbot, *J. Chem. Phys.* **106**, 4696 (1997).
- [16] P. van der Schoot, *J. Chem. Phys.* **106**, 2355 (1997).
- [17] A. Perera, *J. Mol. Liq.* **109**, 73 (2004).
- [18] Y. Martínez-Ratón, E. Velasco, and L. Mederos, *Phys. Rev. E* **72**, 031703 (2005).
- [19] See, e.g., K. J. Strandburg, *Rev. Mod. Phys.* **60**, 161 (1988).
- [20] J. P. Straley, *Phys. Rev. A* **4**, 675 (1971).
- [21] J. Tobochnik and G. V. Chester, *Phys. Rev. A* **27**, 1221 (1983).
- [22] D. Frenkel and R. Eppenga, *Phys. Rev. A* **31**, 1776 (1985).
- [23] M. A. Bates and D. Frenkel, *J. Chem. Phys.* **112**, 10034 (2000).
- [24] M. C. Lagomarsino, M. Dogteron, and M. Dijkstra, *J. Chem. Phys.* **119**, 3535 (2003).
- [25] J. M. Kosterlitz and D. J. Thouless, *J. Phys. C* **6**, 1181 (1973).
- [26] J. Vieillard-Baron, *J. Chem. Phys.* **56**, 4729 (1972).
- [27] J. A. Cuesta and D. Frenkel, *Phys. Rev. A* **42**, 2126 (1990).
- [28] R. F. Kayser and H. J. Raveché, *Phys. Rev. A* **17**, 2067 (1978).
- [29] J. A. Cuesta, C. F. Tejero, and M. Baus, *Phys. Rev. A* **39**, 6498 (1989).
- [30] H. Schlacken, H.-J. Mogel, and P. Schiller, *Mol. Phys.* **93**, 777 (1998).
- [31] Y. Martínez-Ratón, E. Velasco, and L. Mederos, *J. Chem. Phys.* **122**, 064903 (2005).
- [32] K. W. Wojciechowski and D. Frenkel, *Comp. Met. Sci. Tech.* **10**, 235 (2004).
- [33] A. Donev, J. Burton, F. H. Stillinger, and S. Torquato, *Phys. Rev. B* **73**, 054109 (2006).
- [34] Y. Martínez-Ratón, E. Velasco, and L. Mederos, *J. Chem. Phys.* **125**, 014501 (2006).
- [35] V. Narayan, N. Menon, and S. Ramaswamy, *J. Stat. Mech.: Theory Exp.* 2006, P01005.
- [36] Y. Martínez-Ratón, *Phys. Rev. E* **75**, 051708 (2007).
- [37] The situation in three dimensions (parallel hard cubes) is not completely settled. Initial simulations on mixtures of parallel hard cubes on a lattice [38], supported by an off-lattice fundamental-measure theory (FMT) study [39], seemed to indicate evidence for demixing between two fluid phases. A more detailed analysis of a more consistent off-lattice FMT functional [40], and more recently a FMT-based formulation on a lattice [41], conclude that demixing involves one spatially-ordered phase, and that fluid-fluid demixing is metastable. The present state of affairs is therefore similar to that in hard-sphere mixtures.
- [38] M. Dijkstra and D. Frenkel, *Phys. Rev. Lett.* **72**, 298 (1994); M. Dijkstra, D. Frenkel, and J.-P. Hansen, *J. Chem. Phys.* **101**, 3179 (1994).
- [39] J. A. Cuesta, *Phys. Rev. Lett.* **76**, 3742 (1996).
- [40] Y. Martínez-Ratón and J. A. Cuesta, *J. Chem. Phys.* **111**, 317 (1999).
- [41] L. Lafuente and J. A. Cuesta, *Phys. Rev. Lett.* **89**, 145701 (2002).
- [42] A. Buhot and W. Krauth, *Phys. Rev. E* **59**, 2939 (1999).
- [43] M. A. Cotter and D. C. Wacker, *Phys. Rev. A* **18**, 2669 (1978); **18**, 2676 (1978).
- [44] H. L. Scott, Jr., *Phys. Rev. A* **21**, 2082 (1980).
- [45] The excluded volume between a hard rectangle (labeled as 1) and a hard discorrectangle (labeled as 2) is $V_{12}(\phi) = \sigma_1\sigma_2 + L_1\sigma_2 + L_2\sigma_1 |\cos \phi| + L_1L_2 |\sin \phi| + v_1 + v_2$, with $v_1 = L_1\sigma_1$ and $v_2 = L_2\sigma_2 + \pi\sigma_2^2/4$ the areas of the rectangle and the discorrectangle, respectively.
- [46] Recent results for high-order virial coefficients of several two-dimensional hard convex particles can be found in M. Rigby, *Mol. Phys.* **78**, 21 (1993).
- [47] For the implementation of a Fourier expansion, see Ref. [31]; parametrized forms were used in the present work and also in Refs. [18,34].
- [48] R. van Roij and B. Mulder, *J. Chem. Phys.* **105**, 11237 (1998).
- [49] S. DuBois and A. Perera, *J. Chem. Phys.* **116**, 6354 (2002).
- [50] The value of $\kappa=2.62$ mentioned in Ref. [30] corresponds to the value where the $I-N_u$, N_u-N_t and $I-N_t$ spinodals all meet; as explained in Ref. [31], since the latter spinodal line in fact meets a first-order $I-N_u$ transition, the correct value for thermodynamic stability of the tetratic phase is $\kappa=2.21$.
- [51] D. de las Heras, Y. Martínez-Ratón, and E. Velasco (unpublished).